

Characterization of Physical Processes and Secondary Particle Generation in Radiation Dose Enhancement for Megavoltage X-rays

Chulhwan Hwang,¹ JungHoon Kim^{2,*}

¹Departments of Radiology, Masan University

²Departments of Radiological Science, Catholic University of Pusan

Received: June 24, 2019. Revised: August 26, 2019. Accepted: October 31, 2019

ABSTRACT

We evaluated the physical properties that occur to dose enhancement and changes from secondary particle production resulting from the interaction between enhancement material. Geant4 was used to perform a Monte Carlo simulation, and the medical internal radiation dose (MIRD) head phantom were employed. X-rays of 4, 6, 10, 15, 18, and 25 MV were used. Aurum (Au) and gadolinium (Gd) were applied within the tumor volume at 10, 20, and 30 mg/g, and an experiment using soft tissue exclusively was concomitantly performed for comparison. Also, particle fluence and initial kinetic energy of secondary particle of interaction were measured to calculate equivalent doses using the radiation weight factor. The properties of physical interaction by the radiation enhancement material showed the great increased in photoelectric effect as compared to the Compton scattering and pair production, occurred with the highest, in aurum and gadolinium it is shown in common. The photonuclear effect frequency increased as the energy increased, thereby increasing secondary particle production, including alpha particles, protons, and neutrons. During dose enhancement using aurum, a maximum 424.25-fold increase in the equivalent dose due to neutrons was observed. This study was Monte Carlo simulation corresponds to the physical process of energy transmission in dose enhancement. Its results may be used as a basis for future in vivo and in vitro experiments aiming to improve effects of dose enhancement.

Keywords: Dose enhancement, Monte Carlo simulation, Secondary particle

I. INTRODUCTION

Radiation therapy uses high energy (megavoltage or higher) to reduce the integral dose of radiation applied to surrounding normal tissue. Remarkable advances in intensity modulated radiotherapy (IMRT) and volumetric intensity modulated arc radiotherapy (VMAT) have now made it possible to deliver sufficient therapeutic doses while maintaining a low normal tissue complication probability (NTCP).^[1] The ultimate goal of radiation therapy advances is to deliver sufficient therapeutic doses of radiation to tumors and minimize the effects of radiation on surrounding normal tissues. Since the radiation doses

required to improve tumor control probability (TCP) can cause complications in normal tissue depending on the location, pathological features, and systemic conditions of a tumor, care are always needed.^[2,3] Ideally, a high TCP could be maintained with a low probability of complications in normal tissues, and a large difference maintained between the two. This could be achieved by improving the therapeutic ratio (TR).^[4] TR improvement methods include hyperthermia, charged particle therapy, concomitant chemoradiotherapy, and dose enhancement.^[5-8] Dose enhancement increases the cross section of interactions involving substances with high atomic numbers and electronic densities. This increases the number of secondary electrons such as photoelectrons and Auger

* Corresponding Author: JungHoon Kim

E-mail: donald@cup.ac.kr

Tel: +82-10 9142 1171

electrons, thereby increasing local energy transfer.^[9-11] During this process, physical phenomena such as the photoelectric effect, Compton scattering, and pair production occur, and photons with radiation doses of 8-10 MeV or higher can exhibit photonuclear reactions.^[12] Increasing the interaction cross section can increase the linear energy transfer (LET) within a substance and its relative biological effectiveness (RBE), ultimately improved the efficacy of radiation therapy.^[5] Substances such as aurum (Au), gadolinium (Gd), and iodine (I) are used in dose enhancement to account for biological compatibility and chemical safety.^[13-15] Nanoparticles are used to account for enhanced permeability and retention (EPR) within tissues and the vascular system.^[16,17] Dose enhancement effects are reportedly influenced by the substance type, particle size, concentration, and quality of radiation [18]. In-vivo and in-vitro experiments, as well as Monte Carlo simulations investigating dose enhancement have been actively conducted in the last several years.

Although numerous studies have investigated the effects of dose enhancement substances and the determinants of efficacy, research regarding the physical phenomena that occur during dose enhancement and production of secondary particles resulting from these phenomena has been lacking. Therefore, this study aimed to evaluate the physical reactions that occur during dose enhancement, and the resulting production of secondary particles.

II. MATERIAL AND METHODS

Monte Carlo simulations are based on random number sampling and allow three-dimensional (3D) particle transported for various materials and sources. This study conducted a Monte Carlo simulation using geometry and tracking (Geant4, ver. 10.03). A head phantom of the medical internal radiation dose (MIRD) developed by the Oak Ridge National Laboratory (ORND) was converted into a slab and used in the simulation.^[19-20] The head phantom

consisted of a 0.2 cm scalp layer, 0.3 cm soft tissue, 0.9 cm cranium, 11.5 cm brain parenchyma, and tumor tissue-mimicking model with a 2.5 cm radius within the brain parenchyma. Fig. 1 shows the experimental scheme. These constituents adhered to the International Commission on Radiation Units and Measurement (ICRU) report 46.^[21] The simulation used X-rays of 4, 6, 10, 15, 18, and 25 MV and the spectrum of a 2100 C, 2300 C/D medical linear accelerator developed by Varian medical systems, United States.^[22-24] X-rays were vertically irradiated toward the phantom surface from the source 100 cm away. The field size was set to 10×10 cm², and the initial particle transfer was set to 1×10^9 (number of source particle history considering statistical errors). The physics model QGSP_BIC, which includes a standard electromagnetic model, was used. The lower limit of the particle tracking range was set to 1 mm. A mock simulation was performed, including Auger electrons occurring during the deexcitation process within substances.

Aurum and gadolinium were used for describing the dose enhancement substances within the tumor volume at concentrations of 10, 20, and 30 mg/g based on previous reports by Chow et al, Mesbahi et al., and Daniel et al. An experiment using only soft tissues was also performed for comparison.^[25-27] To analyze the physical interactions resulting from dose enhancement within the tumor tissue, changes in the reactions resulting from interactions between the initial particles and dose enhancement substance were measured as ratios according to radiation dose, enhancement substance, and concentration using a sensitive detector by GEANT4. When secondary particles other than electrons arose due to photonuclear reactions, simulation tracking of these secondary particles was performed to identify the particle fluence and initial kinetic energy as well as calculate the equivalent dose from the radiation-weighting factor (W_R) from the International Commission on Radiological Protection (ICRP) publication 103 and 119. The equivalent dose

can be expressed as Eq. (1).

Where H_T is the equivalent dose in Sieverts (Sv) by tissue, W_R is the radiation weighting factor, D_R is the absorbed in grays (Gy) by radiation type R.

$$H_T = \sum W_R \times D_R \quad (1)$$

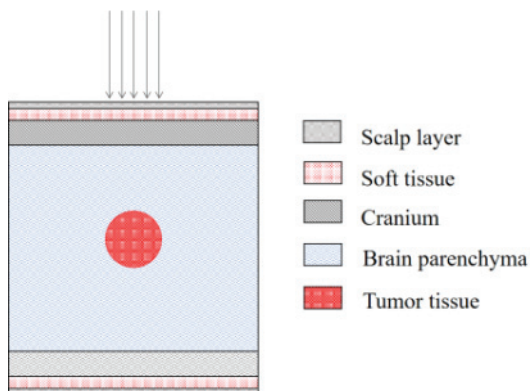


Fig. 1. Geometric diagram of slab head phantom based the MIRD-ORND phantom.

III. RESULT

The physical reactions that occurred during dose enhancement were expressed as ratios of changes in the reactions resulting from interactions between the initial particles and dose enhancement substance. Compton scattering accounted for over 90% of all physical interactions that occurred at 4, 6, 10, 15, 18, and 25 MV within tumor tissues, whereas the photoelectric effect accounted for less than 1%. The frequency of pair production increased as the photon energy increased, and its highest frequency of 7.03% was observed at 25 MV. Photonuclear energy was observed at or over 10 MV, and its frequency increased but remained $<0.1\%$ as irradiation energy increased. Fig. 2 shows physical interactions in tumor. Regarding interaction frequency changes in the relating to dose enhancement, changes in both the photoelectric effect and pair production frequencies, whose interaction cross-section is more significantly affected

by the anatomic number of the dose enhancement substance than that of Compton scattering, were observed. Aurum increased the frequency of the photoelectric effect by 1.59–11.41-fold, that of Compton scattering by 1.13–1.54-fold, that of pair production by 1.18–1.99-fold, and that of photonuclear effect by 1.26–7.23-fold. Gadolinium increased the frequency of the photoelectric effect by 1.00–4.84-fold, that of Compton scattering by 1.05–1.20-fold, that of pair production by 1.08–1.50-fold, and that of photonuclear effect by 1.12–4.57-fold. Increases in these interaction frequencies were more significantly at higher enhancement substance concentrations. Although the frequency of the photoelectric effect, Compton scattering, and pair production did not change according to the amount of photo energy, the photonuclear effect frequency increased as energy increased.

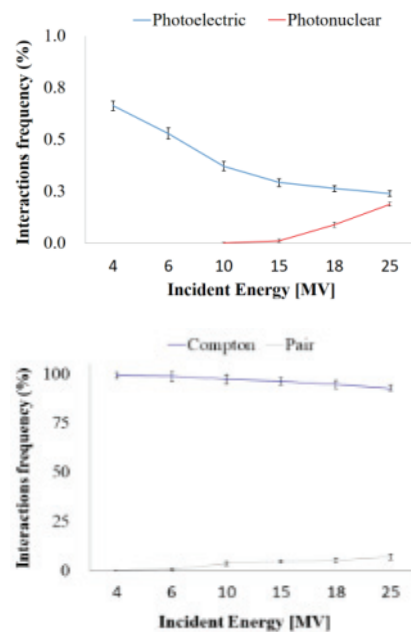


Fig. 2. Frequency of interaction process, (a) photoelectric and photonuclear effect, (b) Compton scattering and pair production in tumour volume according to incident energy. Photonuclear interactions are represented by multiplying by $\times 10$.

A radiation-weighting factor was applied to the fluence, absorbed energy per mass, and initial kinetic energy of the secondary particles that were produced

by the photonuclear effect during interactions with MV X-rays to find the equivalent dose. Particles produced from (γ , α), (γ , p), and (γ , n) reactions within the tumor tissue were tracked. Statistically significant values were obtained for radiation doses of 15 MV X and above. Alpha particles had a fluence of $2.39\text{E-}09 \sim 1.19\text{E-}07 \text{ cm}^{-2}$, protons $5.37\text{E-}09 \sim 8.68\text{E-}08 \text{ cm}^{-2}$, and neutrons $2.77\text{E-}10 \sim 1.35\text{E-}08 \text{ cm}^{-2}$, making their respective equivalent doses $1.07\text{E-}04 \sim 5.93\text{E-}03 \text{ pSv}$, $5.62\text{E-}06 \sim 1.10\text{E-}04 \text{ pSv}$, and $7.35\text{E-}09 \sim 1.60\text{E-}06 \text{ pSv}$. Table 2 shows equivalent dose due to secondary particles. These changes indicated produced particle fluence and equivalent dose increased in response to increases in the photon energy. Alpha particles showed the greatest increase, followed by protons, and then neutrons. Fig. 3 shows particle fluence of secondary particle.

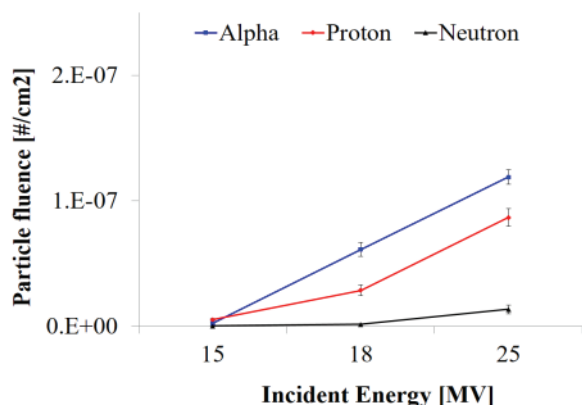


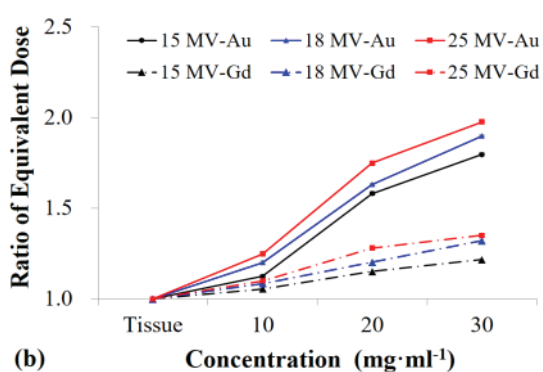
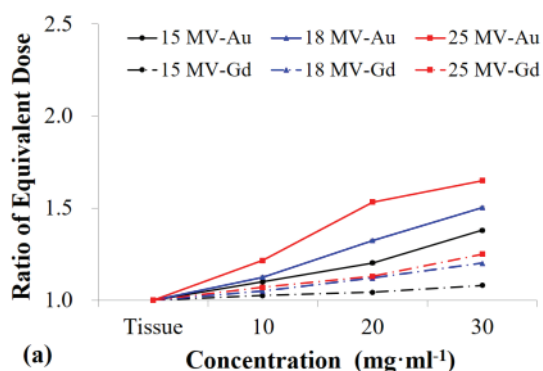
Fig. 3. Fluence of secondary particles according to incident energy from (γ , α), (γ , p), and (γ , n) interactions.

Secondary particle production during dose enhancement indicated an increase in the fluence and equivalent dose resulting from the increased frequency of photonuclear effects. Aurum increased the equivalent dose of alpha particles by 1.09~1.64-fold, protons by 1.12~1.97-fold, and neutrons by 1.42~424.25-fold. Gadolinium increased the equivalent dose of alpha particles by 1.02~1.24-fold, protons by 1.07~1.35-fold, and neutrons by 1.26~2.00-fold. Radiation dose changes due to secondary particle production during

dose enhancement increased as the concentration of enhancement substance and photo energy increased. Additionally, greater dose changes were observed for aurum than gadolinium, with neutrons demonstrating a greater equivalent dose increase than alpha particles and protons. Fig. 4 shows normalized ratios of equivalent dose for dose enhancement through (γ , α), (γ , p), and (γ , n).

Table 1. Equivalent dose, H_T by secondary particles through (γ , α), (γ , p), and (γ , n) interactions.(unit: cm^{-2})

	Secondary particle		
	Alpha	Proton	Neutron
15 MV	1.07E-04	5.26E-06	7.35E-09
18 MV	2.41E-03	4.74E-05	4.43E-08
25 MV	5.93E-03	1.10E-04	1.60E-06



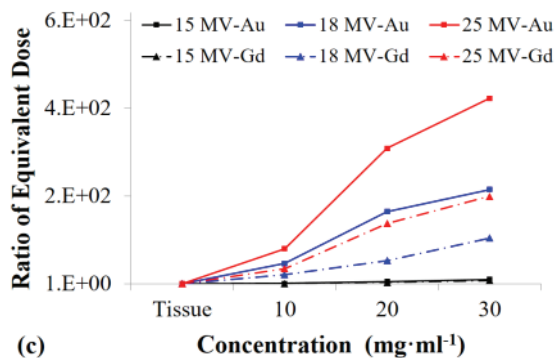


Fig. 4. Normalized ratios of equivalent dose for dose enhancement through (γ, α) , (γ, p) , and (γ, n) interactions: (a) alpha particles, (b) protons, and (c) neutrons.

IV. DISCUSSION

Radiation dose enhancement uses the physical properties of high-atomic number substances to increase radiation doses at local sites without increasing the delivered dose, thereby improving the TCP.^[22] Substances with high atomic numbers such as aurum ($Z=79$, Au), gadolinium ($Z=64$, Gd), and iodine ($Z=53$, I) have been used in numerous studies, and their dose enhancement effects have been observed in in-vitro^[23-25] and in-vivo experiments^[26,27] as well as Monte Carlo simulations.^[28-30] Dose enhancement occurred as a result of the difference in the cross section of the interaction with surrounding substances.^[31] The photoelectric effect is reported to dominate at photon energies in the keV range, and its cross section is affected by the atomic number of the dose enhancement substance.^[12] Dose enhancement substances with high atomic numbers have higher photoelectric absorption coefficients than soft tissue and water (effective atomic numbers (Z_{eff}) 7.22–7.50). Regarding the absorption edges of dose enhancement substances, aurum has a K-edge of 80.7 keV and L-edge of 11.0–14.3 keV, whereas gadolinium has a K-edge of 50.2 keV and L-edge of 7.2–8.3 keV.^[21]

Dose enhancement substances demonstrate higher response coefficients than soft tissues at photo energies in the keV range, and the ratio of the mass attenuation coefficient (μ/ρ) between dose enhancement substances and soft tissues displayed a >100-fold difference at photon energies of 100 keV or less. Conversely, the difference in response coefficients between dose enhancement substances and soft tissues is relatively small (photon energies of 1 MeV or greater) relative to keV-range photon energies. This is because for photon energies at or over MeV, attenuation is predominantly caused by Compton scattering resulting from a substance with a low atomic number. MeV X-ray dose enhancement may thus display more significant differences relative to that of keV X-rays.

Physical interactions that occurred during dose enhancement were analyzed to study the physical reactions caused by dose enhancement substances. These interactions were defined as the initial reactions that occurred within the dose enhancement substance due to the initial photons produced in the Monte Carlo simulation. Due to the energy characteristics of MV X-rays, Compton scattering interactions dominated. The photoelectric effect frequency increased as photon energy decreased, whereas pair production frequency increased as photon energy increased. The photonuclear effect frequency was low at photon energies of 10 MV or higher, but increased as the photon energy increased. The frequency of the photoelectric effect, pair production, and photonuclear effect increased due to the effect of the atomic and nucleic numbers of the dose enhancement substances. No significant changes in Compton scattering frequency were observed. Notably, changes in interaction frequency were more evident in aurum than gadolinium as dose enhancement concentrations increased. These phenomena resulted from changes in the interaction cross sections relating to dose enhancement substances.

Photon energies of MeV or greater that exceed the nuclear binding energy of a substance can lead to the

production of secondary particles such as photoneutrons, photoprotons and photoalphas through (γ , n), (γ , p), (γ , d), and (γ , α) reactions. These reactions can occur within soft tissues, resulting from interactions with carbon, nitrogen, oxygen, and other tissue constituent elements. Secondary particles such as neutrons, protons, and alpha particles exert relatively high biological effects due to LET effects. Allen et al. reported 0.8% and 0.2% dose delivery by photoneutrons at 24 MeV and 30 MeV X-rays, respectively^[28], Ing et al. reported a photoneutron dose of 0.1% at 25 MV X-rays^[29], and Tilikidis et al. reported the maximum photoneutron dose to be 2.0% at 50 MeV X-rays^[30]. This study analyzed the secondary particles resulting from photonuclear effects during dose enhancement, and a radiation-weighting factor obtained from the mean and absorbed particle doses was used to calculate the equivalent dose. Alpha particles, protons, and neutrons released from (γ , n), (γ , p), and (γ , α) reactions were analyzed to assess the production of secondary particles by MV X-rays. The number of produced particles increased as photon energy increased, and the frequency of particle production changed according to the type and concentration of dose enhancement substance. The photonuclear effect, required for secondary particle production, was affected by the number of nucleons constituting the dose enhancement substance and nuclear binding energy.^[28] Increased secondary particle production was observed during dose enhancement with 8.2 and 7.91 MeV binding energies for gadolinium and aurum, respectively. The quantity of secondary particle production and resulting equivalent dose increased as dose enhancement concentration and photon energy increased. Neutrons were produced most frequently, followed by protons and alpha particles. Neutrons showed maximum 424.25-fold and 200.64-fold increases in equivalent dose when aurum and gadolinium were used, respectively. Based on previous reports,^[28-30] neutrons may deliver approximately 0.3–1.5% of the total radiation dose in

dose enhancement. X-rays caused by secondary particles produced within a dose enhancement substance have significant biological effects when not controlled, and can increase the risk of secondary cancer. Therefore, understanding the physical phenomena caused by these particles is meaningful. In this study, a mock simulation of the physical stage of energy transmission was performed for a series of dose enhancement phenomena. These results may be used as basic research materials for future in-vivo and in-vitro dose enhancement experiments.

V. CONCLUSION

Dose enhancement can improve therapeutic ratios by increasing dose absorption at a local site. This study analyzed the physical reactions that occurred during dose enhancement at different MV X-ray doses and the production of secondary particles that result from these reactions. During MV X-ray dose enhancements, the frequencies of the photoelectric effect, pair production, and photonuclear effects were found to be significantly more influenced by the atomic number of the enhancement substance than that of Compton scattering. Secondary particle production from nuclei and inelastic collisions during dose enhancement, as well as the delivered dose, increased as the enhancement substance concentrations and photon energy increased. A notable increase in the equivalent dose due to neutrons was observed during aurum dose enhancement.

Acknowledgement

This research was supported by a Basic Science Research Program through the National Research Foundation of Korea (NRF), funded by the Ministry of Education (2016R1D1A1B03931929).

Reference

- [1] A. Pollack, G. K. Zagars, G. "Starkschal. Prostate

- cancer radiation dose-response: results of the M.D. Anderson Phase III randomized trial," *International Journal of Radiation Oncology, Biology, Physics*, Vol. 53, No. 5, pp. 1097-1105, 2002.
- [2] J. T. Lyman, "Complication probability as assessed from dose-volume histograms," *Radiation Research Supplement*, Vol. 8, No. 1, pp. S13-S19, 1985. Doi: 10.2307/3583506.
- [3] P. Stavrev, N. Stavreva, A. "Niemierko, Generalization of a model of tissue response to radiation based on the ideas of functional subunits and binomial statistics," *Physic in Medicine & Biology*, Vol. 46, No. 5, pp. 1501-1518, 2001.
- [4] A. S. Shiu, D. E. Mellenberg, "General Practice of Radiation Oncology Physics in the 21st Century," *Medical Physics Publishing*, pp. 368, 2000.
- [5] D. Regulla, E. Schmid, W. Friedland, W. Panzer, U. Heinzmann, D. Harder, "Enhanced values of the RBE and H ratio for cytogenetic effects induced by secondary electrons from an X-irradiated gold surface," *Radiation Research*, Vol. 158, No. 4, pp. 505-515, 2002.
- [6] J. E. Sardi, M. A. Boixadera, J. J. Sardi, "A critical overview of concurrent chemoradiotherapy in cervical cancer," *Current Oncology Reports*, Vol. 6, No. 6, pp. 463-470, 2004.
- [7] L. Sim, A. Fielding, M. English, "Enhancement of biological effectiveness of radiotherapy treatments of prostate cancer cells in vitro using gold nanoparticles," *International Nanomedicine Conference*, Coogee Beach, Sydney, pp.14-16, 2011.
- [8] H. P. Kok, J. Crezee, N. A. Franken, "Quantifying the combined effect of radiation therapy and hyperthermia in terms of equivalent dose distributions," *International Journal of Radiation Oncology, Biology, Physics*, Vol. 88, No. 3, pp.739-745, 2014.
- [9] K. T. Butterworth, J. A. Wyer, M. F. Brennan, "Gold nanoparticles: from nanomedicine to nanosensing," *Nanotechnology, Science and Applications*, Vol 2, No 1, pp.45-66, 2008
- [10] E. Brun, L. Sanche, C. Sicard-Roselli, "Parameters governing gold nanoparticle X-ray radiosensitization of DNA in solution," *Colloids and Surfaces B*, Vol. 72, No. 1, pp. 128-134, 2009.
- [11] R. Berbeco, H. Korideck, W. Ngwa, "In vitro dose enhancement from gold nanoparticles under different clinical MV photon beam configurations," *Medical Physics*, Vol. 39, No. 6, pp. 3900-3901, 2012.
- [12] F. M. Khan, *The Physics of Radiation Therapy*. Fourth edition, Wolters Kluwer Lippincott Williams & Wilkins, pp. 592, 2015.
- [13] C. E. Perez-Lopez, H. M. Garnica-Garza, "Monte Carlo modeling and optimization of contrast-enhanced radiotherapy of brain tumour," *Physics in Medicine and Biology*, Vol. 56, No. 13, pp. 4059-4072, 2011.
- [14] D. G. Zhang, V. Feygelman, E. G. Moros, "Monte Carlo study of radiation dose enhancement by gadolinium in megavoltage and high dose rate radiotherapy," *PLOS ONE*, Vol. 9, No. 10, pp. 1-7, 2014.
- [15] P. Retif, S. Pinel, M. Toussaint, "Nanoparticles for radiation therapy enhancement: the key parameters," *Theranostics*. Vol. 5, No. 9, pp. 1030-1045, 2015.
- [16] S. Unezaki, K. Maruyama, J. L. Hosoda, "Direct measurement of the extravasation of polyethyleneglycol-coated liposomes into solid tumor tissue by in vivo fluorescence microscopy," *International Journal of Pharmaceutics*, Vol. 144, No.1, pp. 11-17, 1996.
- [17] H. Maeda, J. Fang, T. Inutsuka, "Enhanced permeability and retention (EPR) effect for anticancer nanomedicine drug targeting," *Methods in Molecular Biology*, Vol. 624, pp. 25-37, 2010.
- [18] A. Mesbahi, F. Jamali, N. Gharehaghaji, "Effect of photon beam energy, gold nanoparticle size and concentration on the dose enhancement in radiation therapy," *Bioimpacts*. Vol. 3, No. 1, pp. 29-35, 2013.
- [19] E. Y. Han, W. Bolch, K. F. Eckerman, "Revisions to the ORNL series of adult and pediatric computational phantoms for use with the MIRD schema," *Health Physics*, Vol. 90, No. 4, pp. 337-356, 2006.
- [20] S. B. Jia, M. H. Hadizadeh, A. A. Mowlavi, M. E. Loushab, "Evaluation of energy deposition and secondary particle production in proton therapy of

- brain using a slab head phantom," *Reports of Practical Oncology and Radiotherapy*, Vol 19, No. 6, pp. 376-384, 2014.
- [21] ICRU. Photon, electron, proton and neutron interaction data for body tissues. ICRU Report 46. Internat Comm Radiation Units and Measurements, Bethesda, MD, 1992.
- [22] D. Sheikh-Bagheri, D. Rogers, "Monte Carlo calculation of nine megavoltage photon beam spectra using the BEAM code," *Medical Physics*. Vol. 29, No. 3, pp. 391-402, 2002.
- [23] A. Baumgartner, A. Steurer, F. J. Maringer, "Simulation of photon energy spectra from Varian 2100 C and 2300C/D Linacs: simplified estimates with PENELOPE Monte Carlo models," *Applied Radiation and Isotopes*, Vol. 67, No. 11, pp. 2007-2012, 2009.
- [24] A. Mesbahi, M. Fix, M. Allahverdi, E. Grein, H. Garaati, "Monte Carlo calculation of Varian 2300C/D Linac photon beam characteristics: a comparison between MCNP4C, GEANT3 and measurements," *Applied Radiation and Isotopes*, Vol. 62, No. 3, pp. 467-477, 2005.
- [25] J. C. Chow, M. K. Leung, D. A. Jaffray, "Monte Carlo simulation on a gold nanoparticle irradiated by electron beams," *Physics and Medicine and Biology*, Vol. 57, No. 11, pp. 3323-3354, 2012.
- [26] G. Daniel, F. Vladmir, G. Eduardo, "Monte Carlo study of radiation dose enhancement by gadolinium in megavoltage and high dose rate radiotherapy," *PLOS ONE*, Vol. 9, No. 10, pp. 1-7, 2014.
- [27] A. Mesbahi, F. Jamali, N. Gharehaghaji, "Effect of photon beam energy, gold nanoparticle size and concentration on the dose enhancement in radiation therapy," *BioImpacts*. Vol. 3, No. 1, pp. 29-35, 2013.
- [28] P. D. Allen, M. A. Chaudhri. "Charged photoparticle production in tissue during radiotherapy," *Medical Physics*. Vol. 24, No. 6, pp. 837-839, 1997.
- [29] H. Ing, W. R. Nelson, R. A. Shore, "Unwanted photon and neutron radiation resulting from collimated photon beams interacting with the body of radiotherapy patients," *Medical Physics*, Vol. 9, No. 1, pp. 27-33, 1982.
- [30] A. Tilikidis, B. Lind, P. Nafstadius, A. Brahme, "An estimation of the relative biological effectiveness of 50 MV scanned bremsstrahlung beams by microdosimetric techniques," *Physics in Medicine and Biology*, Vol. 41, No. 1, pp. 55-69, 1996.
- [31] K. T. Butterworth, S. J. McMahon, L. E. Taggart, Prise KM. "Radiosensitization by gold nanoparticles: effective at megavoltage energies and potential role of oxidative stress," *Translation Cancer Research*, Vol. 2, No 4, pp. 269-279, 2013.

MV X선의 방사선 선량 증강 현상에서 물리적 특성과 이차입자의 발생

황철환,¹ 김정훈^{2,*}

¹마산대학교 방사선과

²부산가톨릭대학교 방사선학과

요 약

선량 증강 현상에서 발생하는 물리적 특성과 증강 물질과의 상호 작용으로부터 발생하는 이차입자 생성을 평가하였다. Geant 4, MIRD 두부 팬텀을 이용한 몬테카를로 전산 모사를 진행하였으며, 선형가속기에서 발생하는 4, 6, 10, 15, 18, 25 MV X선을 선원으로 적용하였다. 10, 20, 30 mg/g의 금(aurum), 가돌리늄(gadolinium) 증강 물질을 팬텀 내부 종양에 모사하였으며, 물리적 상호작용의 변화와 이차입자 발생에 따른 입자 플루언스와 초기 에너지로부터 방사선가중인자를 고려하여 등가선량을 평가하였다. 방사선 선량 증강 물질에 의한 상호작용은 고 원자번호에서 기인하여 광전효과에 의한 에너지 흡수를 높이는 것으로 나타났으며, 10 MV 이상의 에너지에서는 광핵반응의 증가를 나타내었다. 이로 인해, 팬텀 내부에서 양성자와 중성자와 같은 이차입자 발생의 증가를 보였으며, 중성자에 의한 등가선량이 최대 424.2배 증가하는 것으로 나타났다. 본 연구는 선량 증강 현상에서의 에너지 전달, 흡수의 물리적 과정을 모사하여, 증강 현상에서 발생하는 물리적 특성을 분석하고자 하였다. 이러한 결과는 향후 *in-vivo*, *in-vitro* 선량 증강 실험을 위한 기초 자료로 활용될 수 있을 것으로 사료된다.

중심단어: 몬테칼로 시뮬레이션, 방사선 선량 증강, 이차입자 발생.

연구자 정보 이력

	성명	소속	직위
(제1저자)	황철환	마산대학교 방사선과	교수
(교신저자)	김정훈	부산가톨릭대학교 방사선학과	교수